

BIOPHOTONICS

PACS numbers: 87.63.lt; 87.64.Cc; 87.57.Q–
DOI: 10.1070/QE2013v043n10ABEH014930

Dynamic OCT monitoring and quantification of light penetration enhancement for normal, benign and cancerous human lung tissues at different concentrations of glycerol

Shu-wen Tan, Ying Jin, Hui Yu, Guo-yong Wu

Abstract. **We have evaluated the dynamic effects of the analyte diffusion on the 1/e light penetration depths of normal, benign and cancerous human lung tissue *in vitro*, as well as have monitored and quantified the dynamic change in the light penetration depths of the mentioned human lung tissue after application of 25% and 50% glycerol solution, respectively. The light penetration depths of the analyte diffusion in the lung tissue are measured using the Fourier-domain optical coherence tomography (FD-OCT). Experimental results show that the application of glycerol as a chemical agent can significantly enhance light penetration depths into the human normal lung (NL), lung benign granulomatosis (LBG) and lung squamous cell carcinoma (LSCC) tissue. In-depth transport of the glycerol molecules in the NL, LBG and LSCC tissue at a lower glycerol concentration (25%) are faster than those at a higher glycerol concentration (50%), and the 1/e light penetration depths at a lower glycerol concentration (25%) are smaller than those at a higher glycerol concentration (50%), respectively. Their differences in the maximal 1/e light penetration depths of the NL, LBG and LSCC tissue at a higher and a lower glycerol concentrations were only 8.8%, 6.8% and 4.7%, respectively.**

Keywords: *glycerol diffusion, light penetration depth, human lung tissue, human diseased lung tissue, Fourier-domain optical coherence tomography.*

1. Introduction

Visible, near-IR and UV light have been extensively used in phototherapeutic and diagnostic techniques [1–4]. However, the light penetration depth is still limited to a few centimeters, due to the highly scattering nature of human tissue, which prevents the deeper microstructures from imaging. In order to enhance the imaging depth for the current high resolution optical imaging techniques, the light scattering in tissue must be reduced [5]. Biological tissues are optically inhomogeneous and absorbing media. When imaging with near-IR light, the dominant process that limits the imaging depth and contrast is scattering rather than absorption. It is well documented that light scattering is determined by the size, position and shape of the scatterers relative to the wavelength of incident light [6]. As a consequence, in order to enhance the light penetration depth through the human tissue, the tissue scattering must be reduced for the time of the diagnostic period, i.e. for this period the upper tissue layers should be optically transparent [6]. The turbidity of a dispersive physical system can be effectively controlled by using the optical immersion method based on the concept of matching of refractive indices of scatterers and ground material [7–9]. This technique, which is well known in dispersive optics of physical systems, and was successfully applied in 1950–1970 to cell and microorganism phase microscopy studies [7–12], can be considered as a new approach for tissue optics, especially for contrasting of images of a living tissue and getting more precise spectroscopic information from tissue depth [13–23]. Another possibility to control optical properties of a disperse system is to change its packing parameter and/or scatterer sizing, which is also in use in tissue optics [10, 11]. *In vivo* control of tissue optical properties is important for many biomedical applications [7–9]. The selective translucence of the upper tissue layers is a key technique for the structural and functional imaging, particularly for detection of local static or dynamic inhomogeneities hidden by a highly scattering medium. A significant reduction of scattering by optical immersion of a bulk tissue by means of intra-tissue administration of the appropriate chemical agent has been demonstrated in [5–9].

Lung cancer is the leading cause of cancer-related mortality worldwide, with nearly 1.4 million deaths each year [24–26]. Of the 1.6 million new cases of lung cancer diagnosed each year, approximately 220000 are diagnosed in the United States [27]. There has been an overall decrease in the incidence of lung cancer in men, although in women this trend has only been noted very recently in the United States. In contrast, in many parts of the world the number of cases and deaths related to lung cancer is on the rise [24]. It is also increasingly becoming a disease of the elderly, with a median age at diagnosis of approximately 70 years [28]. Lung cancer is diagnosed at an advanced stage in a majority of patients, which is the primary reason behind the high mortality rate associated with this disease. However, early detection of lung cancer is important and vital for the patient.

Shu-wen Tan College of Biophotonics, South China Normal University, Guangzhou 510631, Guangdong Province, China; Chinese Medicine & Photonic Techniques Three Grade Laboratory of State Administration of Traditional Chinese Medicine, Guangzhou 510631, Guangdong Province, China; Department of Animal Science, Foshan University, Nanhai 528231, Guangdong Province, China;
Ying Jin College of Biophotonics, South China Normal University, Guangzhou 510631, Guangdong Province, China; Chinese Medicine & Photonic Techniques Three Grade Laboratory of State Administration of Traditional Chinese Medicine, Guangzhou 510631, Guangdong Province, China; e-mail: jinying@scnu.edu.cn;
Hui Yu Department of Animal Science, Foshan University, Nanhai 528231, Guangdong Province, China;
Guo-yong Wu Department of Surgery, the First Affiliated Hospital, Sun Yat-Sen University, Guangzhou 510080, Guangdong Province, China

Received 13 June 2012; revision received 24 December 2012
Kvantovaya Elektronika **43** (10) 974–978 (2013)
Submitted in English

A few studies have demonstrated that the depth of light penetrations of various biotissues can be effectively increased by using the optical clearing agents (OCAs), such as the glycerol [29–31], glucose [32, 33], dimethyl sulfoxide [34–36], etc. Several imaging techniques have been used to study the permeation of analytes in biological tissues [37], including ultrasound [38], magnetic resonance imaging (MRI) [39], optical projection tomography (OPT) [40], and optical coherence tomography (OCT) [41–46]. OCT is particularly attractive: Being a nondestructive, noninvasive technique, it provides high-resolution, real-time images of biological tissues. OCT has been used extensively in tissue studies [41–46]. The method has been used to measure permeation of different molecules and materials through various epithelial tissues such as rabbit sclera [42], monkey skin [43], rabbit cornea [44], porcine aorta [43, 45, 46], human skin [47] and human esophagus [48]. OCT penetration depth is on the order of 1–2 mm [49]. Although the imaging depth of OCT is better than that of light microscopy, limitations exist due to the fact that most biological tissues strongly scatter the probing light within the visible and near-IR range, i.e., the therapeutic optical window. The optical immersion method (optical clearing method) is often used to reduce scattering by topical applications of biocompatible chemical agents. The optical clearing technique can be result to deeper penetration of light into tissues by using the OCAs [4–6].

In this study, the hyperosmotic agents of 25% and 50% glycerol have been applied in human normal lung (NL), lung benign granulomatosis (LBG) and lung squamous cell carcinoma (LSCC) tissues to achieve higher resolution and imaging depth of OCT. We monitor and quantify the differences in the light penetration depths of 25% and 50% glycerol diffusion by using the OCT in human NL, LBG and LSCC tissues *in vitro*, respectively.

2. Materials and methods

The experiments were performed by using a Fourier-domain optical coherence tomography (FD-OCT) system. A schematic of the OCT system is shown elsewhere [50]. A broadband superluminescent diode (SLD) light source that delivered an output power of 5 mW at a centre wavelength of 830 nm with a bandwidth of 40 nm is used in the FD-OCT system. The SLD radiation is coupled into an optical fibre based on a Michelson interferometer and split by a 50/50 optical fibre coupler. Fifty percent of the light is directed to the reference arm of the interferometer. The residual light is directed towards the resected lung sample, with a focusing optics. A high resolution motorised translation stage accurately controls mirror movement. Light backscattered from the imaged sample is combined with light reflected from the reference arm and produces an interference signal only if the optical path length difference between the two beams is within the coherence length of the SLD. The combined back-reflected sample and reference light is detected by a spectrometer together with an array detector (usually a CCD camera) [51]. This FD-OCT system provides an axial resolution of around 12 μm and the transverse resolution of about 15 μm. The system signal-to-noise ratio measures 120 dB. The OCT system operation is controlled automatically by the computer. The scanning rate of the current system is 2000 scans per second. The data acquisition software is written in Lab-VIEW 7.2-D environment. Two-dimensional (2D) OCT images are obtained in each experiment and stored in the computer for further processing.

In vitro experiments were performed with human NL, LBG and LSCC tissue. A total of 24 samples of surgically resected human lung tissues were obtained from patients whose consents were obtained for the study at the First Affiliated Hospital of Sun Yat-Sen University. The samples were divided into three groups according to histological diagnosis: NL tissue (8 samples), LBG tissue (8 samples) and LSCC tissue (8 samples). Each removed tissue section was immersed in a 0.9% sodium chloride solution as soon as possible after the resection and then placed on ice and transported to the laboratory for performing measurements. They were stored at –70 °C until the measurement *in vitro*. Each tissue was cut into pieces of approximately 2.5×2.5 cm in size and placed into physiological saline solution for each OCT measurement.

Glycerol was purchased from the Tianjin Damao Chemical Reagent Factory (Tianjin, China). In the experiments, use was made of 25% and 50% glycerol solutions through mixing the agents with purified and distilled water. Solution of 25% or 50% glycerol was applied to the surface of each tissue of three different lung tissue types, respectively. OCT images were continuously acquired from each lung sample for about 120 min. Right before OCT experiments, the tissues were left at room temperature for 30 min. The lung sections were kept moist by phosphate buffered saline to avoid dehydration and the optical probe was never in contact with the sample during the scanning process. The position of the probe beam on the scanned tissue was monitored using a visible light guiding beam. The selected region of the samples was imaged for about 8 to 10 min before the addition of glycerol solution to record a baseline, and then 25% or 50% glycerol solution was applied to the surface of lung specimens for 15 min. The solutions were removed prior to OCT imaging. Every 30 min during the measurement, glycerol solution was applied again on the tissue for 5 min. Then the OCT imaging was continuously monitored for about 2 hours. And the room temperature was maintained at 22 °C throughout the entire experiment. No tissues were used in more than one experiment.

Freezing certainly cause changes in the tissue structure. Depending on the cooling or thawing rates and the final frozen temperature, both extracellular and intracellular ice can be produced. Extracellular ice formation may cause cellular dehydration as a result of the changes in the solute concentration of the cellular constituents. This may cause proteins to lose their tertiary and quartenary structures, resulting in tissue denaturation. Intracellular ice formation may induce mechanical injury as a result of ice crystallisation that damages the cell walls [52]. The effects of cryopreservation on human aorta optical properties have been studied by Cilesiz and Welch [53]. Their results suggest that freezing introduces a significant decrease in the absorption coefficient from 300 nm to 800 nm. Our study is to compare the differences in the light penetration depths of thawed lung tissue of different type after application of 25% and 50% glycerol solution by using the OCT *in vitro*.

OCT images of these lung samples were processed using an original program developed in Matlab program to obtain OCT signals, and then the quantitative data were obtained by averaging the linear signal intensity across the lateral imaging range as a function of depth. Light penetration depths in the human NL, LBG and LSCC tissue were found by using a best fit exponential curve describing well the averaged and normalised signal intensity data [54, 55]. Due to the increase in the in-depth concentration, the light scattering coefficient is altered. The changes in the optical properties were shown in biological tissues through time induced by the glycerol diffusion.

3. Results and discussion

Figure 1a and 2a show the relative 1/e light penetration depth as a function of time recorded from human NL tissue after application of 25% and 50% glycerol solution. The behaviour of the penetration depth in the NL tissue during 25% glycerol diffusion is similar to that during 50% glycerol diffusion. It can be seen from Fig. 1a and Fig. 2a that the relative 1/e light penetration depths in native NL tissue are relatively constant in the time interval from 0 to 10 min. In both cases, mean light penetration depths are about 0.68 mm. The light penetration depth in the NL tissue after the application of 25% glycerol solution gradually increases in the time range from 10 to 72 min, achieving a maximum value of about 0.82 mm at 72 min, and then decreasing to about 0.74 mm at 120 min. Similarly, the light penetration depth in the NL tissue after the application of 50% glycerol solution also gradually increases in the time interval from 10 to 108 min, achieving a maximum value of about 0.88 mm at 108 min, and then gradually decreasing down to about 0.86 mm at 120 min.

Figures 1b and 2b present the relative 1/e light penetration depth as a function of time recorded from human LBG tissue after application of 25% and 50% glycerol solution and

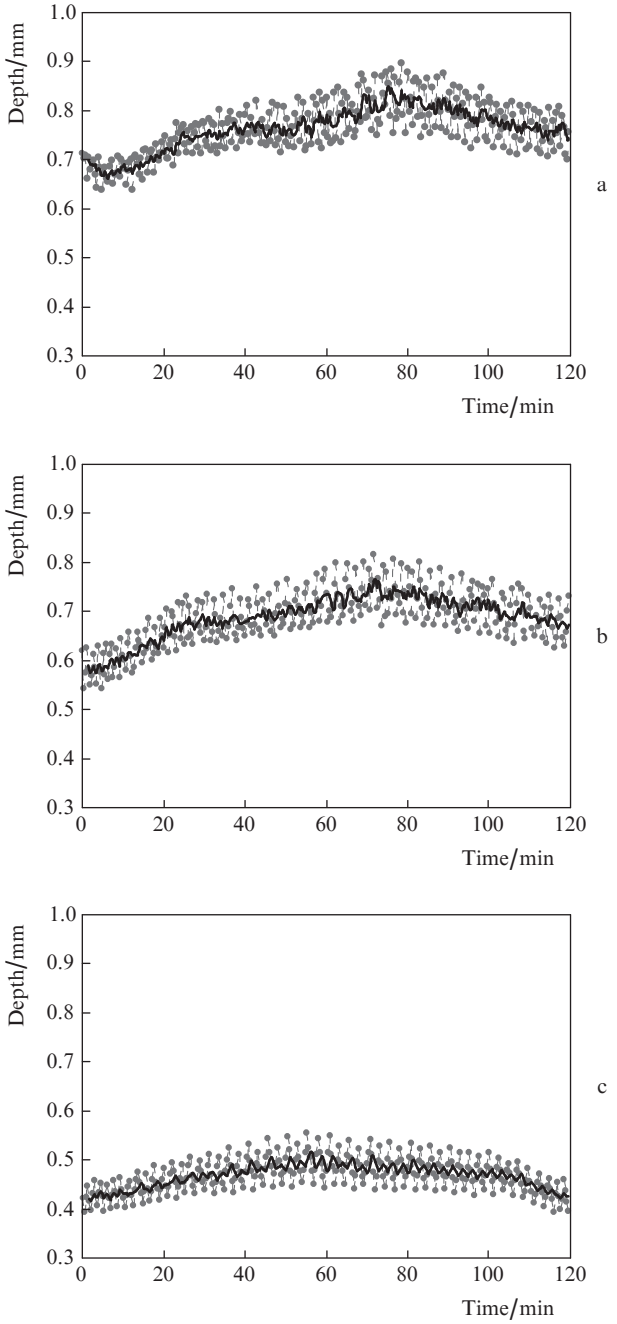

Figure 1. Light penetration depth (at the 1/e level) as a function of time recorded from (a) NL tissue, (b) LBG tissue and (c) LSCC tissue upon 25% glycerol diffusion. Solid curves are the result of averaging of the experimental data.

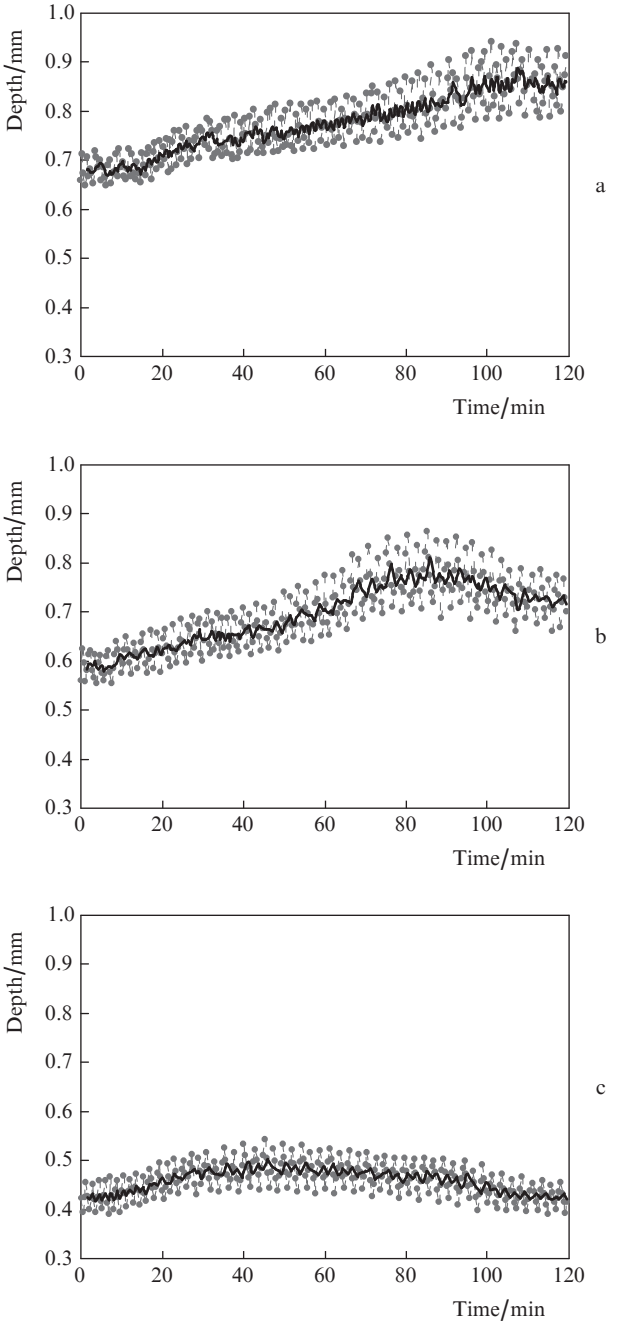

Figure 2. Light penetration depth (at the 1/e level) as a function of time recorded from (a) NL tissue, (b) LBG tissue and (c) LSCC tissue upon 50% glycerol diffusion. Solid curves are the result of averaging of the experimental data.

Figs 1c and 2c show similar dependences for the LSCC tissue. These dependences resemble those in Figs 1a and 2a.

In Figs 1b and 2b, the mean light penetration depth of LBG tissue before application of 25% or 50% glycerol diffusion is about 0.59 mm, moreover the maximal 1/e light penetration depth after the application of 25% glycerol solution is about 0.75 mm at 69 min, and that after the application of 50% glycerol solution is about 0.79 mm at 84 min.

One can see from Figs 1c and 2c that the relative 1/e light penetration depth in the human LSCC tissue before application of 25% and 50% glycerol solution is about 0.42 mm, whereas the maximal 1/e light penetration depth after application of 25% glycerol solution is about 0.50 mm at 56 min, and that after application of 50% glycerol solution is about 0.52 mm at 43 min.

The maximal light penetration depth indicated the elimination of the refractive index mismatch in the NL, LBG and LSCC tissue, which made it possible to conclude that the diffusion of glycerol had ceased or reached an equilibrium state. The subsequent decrease in the maximal light penetration depth, observed for all the tissues in question, could be the result of a reverse process in the tissue where water begins to return in the interior of the tissue [33].

The experimental results indicated that the in-depth transport of glycerol molecules in the NL, LBG and LSCC tissue at a lower glycerol concentration (25%) were faster than those at a higher glycerol concentration (50%), and the 1/e light penetration depths in the first case were smaller than those in the second case. The differences in glycerol diffusion rates in the NL, LBG and LSCC tissue after application of different glycerol concentrations are explained by the fact that glycerol of higher concentration has a greater viscosity than glycerol of lower concentration [7]. However, the differences in the maximal 1/e light penetration depths in the NL, LBG and LSCC tissue at a high (50%) and a low (25%) glycerol concentrations were only 8.8%, 6.8% and 4.7%, respectively. These differences are related to the differences in the refractive indices of the analytes solutions.

The highly scattering nature of the human tissue limits the light penetration depth in the near-IR range. However, the major source of scattering in tissues and cell structures is the refractive index mismatch between mitochondria, cytoplasm, cell membrane, extracellular media, and its components such as collagen and elastin fibres [18]. The turbidity of a dispersive physical system can be effectively reduced using the immersion effect – matching of refractive indices of the scatterers and the ground material due to its impregnation by an agent with a higher refractive index. The refractive index matching of components of a highly scattering tissue has a strong influence on tissue transmittance and reflectance, as well as polarisation and coherence of scattered light [56].

The results obtained also show that the increase in the local in-depth glycerol concentration results in an increase in the light penetration depths of the NL, LBG and LSCC tissue during the diffusion process, but their increments are markedly different. Figures 1 and 2 indicate that before application of glycerol solution, the 1/e light penetration depth in the NL tissue was 1.15 times higher than a similar quantity of the LBG tissue, which in turn exceeded by 1.41 times that of the LSCC tissue. After application of 25% glycerol solution, the maximal increments in the 1/e light penetration depths of NL, LBG and LSCC tissue were 1.25, 1.27 and 1.19 times higher as compared to their counterparts before application of 25% glycerol solution. After application of 50% glycerol solution, the maximal increments in the 1/e light penetration depths of NL, LBG and LSCC tissue were 1.29, 1.34 and 1.24 times higher than their counterparts before application of the solution. Therefore, application of hyperosmotic agents has a potential to become a useful tool for the enhancement of penetration depth of optical imaging modalities including OCT. Our future studies will focus on more accurate measurements of changes in optical properties of human lung tissues through application of OCAs.

4. Conclusions

We have demonstrated that application of glycerol as a chemical agent can significantly enhance light penetration depths into the NL, LBG and LSCC tissue. The results indicate that the in-depth transport of glycerol molecules in the NL, LBG and LSCC tissue at a lower glycerol concentration (25%) was faster than that at a higher concentration (50%), and the 1/e light penetration depths in the first case were smaller that in the second one. The maximal 1/e light penetration depths in the NL, LBG and LSCC tissue at higher (50%) and a lower (25%) glycerol concentrations differed only by 8.8%, 6.8% and 4.7%, respectively. Our experiments demonstrate that the increase in the local in-depth glycerol concentration resulted in the increase in the 1/e light penetration depths of the NL, LBG and LSCC tissue during the diffusion process, but their increments are markedly different. This might potentially be diagnosed by comparing the 1/e light penetration depths of several therapeutic or diagnostic agents in the NL, LBG and LSCC tissue. Therefore, dynamic monitoring and precise assessment of the diffusion processes in the NL, LBG and LSCC tissue with the help of OCT might provide a truly effective way for evaluating the tissue health.

Acknowledgements. This work was supported by the National Natural Science Foundation of China (Grant Nos 30940020 and 81171379).

References

1. Kawada A., Aragane Y., Kameyama H., Sangen Y., Tezuka T. *J. Dermatol. Sci*., **30**, 129 (2002).
2. Lee S.Y., You C.E., Park M.Y. *Lasers Surg. Med*., **39**, 180 (2007).
3. Donohoe A., Hare N.O., Barnes L. *Ir. J. Med. Sci*., **171**, 94 (2002).
4. Kwon K., Son T., Lee K.J., Jung B. *Lasers Med. Sci.*, **24**, 605 (2009).
5. Wang R.K., Tuchin V.V. *J. X-Ray Sci. Technol.*, **10**, 167 (2002).
6. Xu X.Q., Zhu Q.H. *Opt. Commun.*, **279**, 223 (2007).
7. Tuchin V.V. *Laser Phys.*, **15**, 1109 (2005).
8. Genina E.A., Bashkatov A.N., Tuchin V.V. *Expert Rev. Med. Devices*, **7**, 825 (2010).
9. Tuchin V.V. *J. Phys. D: Appl. Phys*., **38**, 2497 (2005).
10. Barer R., Ross K.F.A., Tkaczyk S. *Nature*, **171**, 720 (1953).
11. Barer R., Joseph S. *Q. J. Microsc. Sci.*, **95**, 399 (1954).
12. Fikhman B.A. *Mikrobiologicheskaya refraktometriya* (Microbiological Refractometry) (Moscow: Medicine, 1967).
13. Rol P., Neiderer P., Durr U., Henchoz P.D., Frankhauser F. *Ophthalmic Surg. Lasers*, **3**, 201 (1990).
14. Tuchin V.V. *J. Laser Appl*., **5**, 43 (1993).
15. Chance B., Liu H., Kitai T., Zhang Y. *Anal. Biochem*., **227**, 351 (1995).
16. Liu H., Beauvoit B., Kimura M., Chance B. *J. Biomed. Opt.*, **1**, 200 (1996).
17. Tuchin V., Maksimova I., Zimnyakov D., Kon I., Mavlutov A., Mishin A. *Proc. SPIE Int. Soc. Opt. Eng.*, **2925**, 118 (1996).
18. Tuchin V.V., Maksimova I.L., Zimnyakov D.A., Kon I.L., Mavlutov A.H., Mishin A.A. *J. Biomed. Opt*., **2**, 401 (1997).
19. Tuchin V.V., Culver J., Cheung C., Tatarkova S.A., Della Vecchia M.A., Zimnyakov D., Chaussky A., Yodh A.G., Chance B. *Proc. SPIE Int. Soc. Opt. Eng.*, **3598**, 111 (1999).

20. Bashkatov A.N., Tuchin V.V., Genina E.A., Sinichkin Yu.P., Lakodina N.A., Kochubey V.I. *Proc. SPIE Int. Soc. Opt. Eng.*, **3591**, 311 (1999).
21. Vargas G., Chan E.K., Barton J.K., Rylander H.G. III, Welch A.J. *Laser. Surg. Med.*, **24**, 133 (1999).
22. Tuchin V.V. *Proc. SPIE Int. Soc. Opt. Eng.*, **4001**, 30 (2000).
23. Tuchin V.V. *Proc. SPIE Int. Soc. Opt. Eng.*, **4224**, 351 (2000).
24. Jemal A., Center M.M., Desantis C., Ward E.M. *Cancer Epidemiol. Biomarkers Prev*., **19**, 1893 (2010).
25. Ramalingam S.S., Owonikoko T.K., Khuri F.R. *CA Cancer J. Clin*., **61**, 91 (2011).
26. Hurria A., Kris M.G. *CA Cancer J. Clin*., **53**, 325 (2003).
27. Jemal A., Siegel R., Xu J., Ward E. *CA Cancer J. Clin*., **60**, 277 (2010).
28. Owonikoko T.K., Ragin C.C., Belani C.P., Oton A.B., Gooding W.E., Taioli E., Ramalingam S.S. *J. Clin. Oncol.*, **25**, 5570 (2007).
29. Jiang J., Boese M., Turner P., Wang R.K. *J. Biomed. Opt*., **13**, 021105 (2008).
30. Zhu D., Zhang J., Cui H., Mao Z.Z., Li P.C., Luo Q.M. *J. Biomed. Opt*., **13**, 021106 (2008).
31. Mcnichols R.J., Fox M.A., Gowda A., Tuya S., Bell B., Motamed M. *Lasers Surg. Med.*, **36**, 289 (2005).
32. Ghosn M.G., Tuchin V.V., Larin K.V. *Opt. Lett*., **31**, 2314 (2006).
33. Ghosn M.G., Sudheendran N., Wendt M., Glasser A., Tuchin V.V., Larin K.V. *J. Biophotonics*, **3**, 25 (2010).
34. Zimmerley M., Mcclure R.A., Choi B., Potma E.O. *Appl. Opt*., **48**, D79 (2009).
35. He Y., Wang R.K. *J. Biomed. Opt*., **9**, 200 (2004).
36. Otter W.K., Notman R., Anwar J., Noro M.G., Briels W.J. *Chem. Phys. Lipids*, **154**, S2 (2008).
37. Ghosn M.G., Mashiatulla M., Syed S.H., Mohamed M.A., Larin K.V., Morrisett J.D. *J. Lipid Res*., **52**, 1429 (2011).
38. Goldberg B.B. *Clin. Diagn. Ultrasound*, **28**, 35 (1993).
39. Uematsu H., Maeda M., Sadato N., Matsuda T., Ishimori Y., Koshimoto Y., Yamada H., Kimura H., Kawamura Y., Hayashi N., Yonekura Y., Ishii Y. *Radiology*, **214**, 912 (2000).
40. Ripoll J., Meyer H., Garofalakis A. *Opt. Mater*., **31**, 1082 (2008).
41. Larin K.V., Tuchin V.V. *Kvantovaya Elektron*., **38**, 551 (2008) [*Quantum Electron*., **38**, 551 (2008)].
42. Ghosn M.G., Carbajal E.F., Befrui N.A., Tuchin V.V., Larin K.V. *J. Biomed. Opt*., **13**, 021110 (2008).
43. Ghosn M.G., Leba M., Vijayananda A., Rezaee P., Morrisett J.D., Larin K.V. *J. Biophotonics*, **2**, 573 (2009).
44. Ghosn M.G., Tuchin V.V., Larin K.V. *Invest. Ophthalmol. Vis. Sci*., **48**, 2726 (2007).
45. Ghosn M.G., Carbajal E.F., Befrui N.A., Tellez A., Granada J.F., Larin K.V. *J. Biomed. Opt*., **13**, 010505 (2008).
46. Ghosn M.G., Syed S.H., Befrui N.A., Leba M., Vijayananda A., Sudheendran N., Larin K.V. *Laser Phys*., **19**, 1272 (2009).
47. Guo X., Guo Z.Y., Wei H.J., Yang H.Q., He Y.H., Xie S.S., Wu G.Y., Deng X.Y., Zhao Q.L., Li L.Q. *Photochem. Photobiol.*, **87**, 734 (2011).
48. Zhao Q.L., Si J.L., Guo Z.Y., Wei H.J., Yang H.Q., Wu G.Y., Xie S.S., Li X.Y., Guo X., Zhong H.Q., Li L.Q. *Laser Phys. Lett*., **8**, 71 (2011).
49. Schmitt J.M. *IEEE J. Sel. Top. Quantum Electron*., **5**, 1205 (1999).
50. Guo X., Wu G.Y., Wei H.J., Deng X.Y., Yang H.Q., Ji Y.H., He Y.H., Guo Z.Y., Xie S.S., Zhong H.Q., Zhao Q.L., Zhu Z.G. *Photochem. Photobiol*., **88**, 311 (2012).
51. Yang Y., Bagnaninchi P.O., Whiteman S.C., Pittius D.G., Elhaj A.J., Spiteri M.A., Wang R.K. *J. Phys. D: Appl. Phys*., **38**, 2590 (2005).
52. Chan E., Menovsky T., Welch A.J. *Appl. Opt*., **35**, 4526 (1996).
53. Cilesiz I.F., Welch A.J. *Lasers Surg. Med*., **14**, 396 (1994).
54. Stumpp O., Chen B., Welch A.J. *J. Biomed. Opt.*, **11**, 041118 (2006).
55. Xu X.Q., Zhu Q.H. *IEEE J. Sel. Top. Quantum Electron*., **14**, 56 (2008).
56. Tuchin V.V. *J. Biomed. Opt*., **4**, 106 (1999).